First-Principle Analysis of the IR Stretching Band of Liquid Water

3 AUTHORS:

Cui Zhang
Princeton University
14 PUBLICATIONS **237** CITATIONS

SEE PROFILE

Davide Donadio
University of California, Davis
109 PUBLICATIONS **4,020** CITATIONS

SEE PROFILE

Giulia Galli
University of California, Davis
**452** PUBLICATIONS **12,484** CITATIONS

SEE PROFILE

First-Principle Analysis of the IR Stretching Band of Liquid Water

Cui Zhang,*,[†] Davide Donadio,[†] and Giulia Galli[‡,†]

[†]Department of Chemistry and [‡]Department of Physics, University of California, Davis, California 95616

ABSTRACT We provide an interpretation of the complex shape of the infrared (IR) stretching band of neat, heavy water, based on the results of ab initio molecular dynamics simulations. We show that intermolecular dipolar correlations play a key role in determining the shape and width of the band and that these correlations are long-ranged, extending to the second coordination shell. Both hydrogen-bonded and non-hydrogen-bonded molecules contribute to the IR stretching band over the entire frequency range, with no distinctive peak or shoulder associated with each species. Within a molecular orbital picture, we identified specific features of the band arising from correlations of electronic contributions to the IR activity.

SECTION Kinetics, Spectroscopy
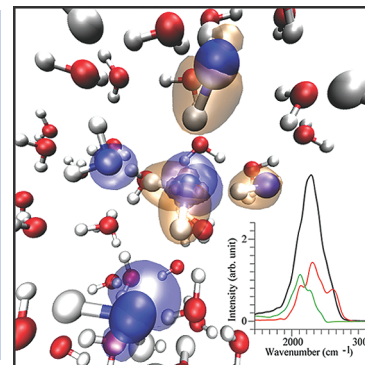
In the last several decades, vibrational spectroscopy has been widely used to probe the structure and dynamics of water, and much progress has been reported about the understanding of hydrogen bonding in the liquid based on two-dimensional (2D) IR spectroscopy.[1] However, despite experimental and theoretical advances, e.g. the interpretation of IR and 2D-IR spectra provided by several simulation studies,[2−7] a detailed understanding of the IR line shapes of liquid water has not yet been achieved.

Most theoretical studies have focused on the OD(OH) dynamics of dilute HOD in $H_2O(D_2O)$, thus providing little information on the effect and range of intermolecular interactions in determining the IR spectrum of neat water. Indeed, in dilute mixtures, OD(OH) frequencies are largely decoupled from those of the remaining molecules in the $H_2O(D_2O)$ liquid. The key contribution of intermolecular dipole−dipole correlations to the IR spectrum of neat D_2O, over the entire spectral range, was recently pointed out by Chen et al.,[4] who, however, did not report any specific analysis of the OD stretching band. On the other hand, this band has been investigated in great detail in dilute mixtures, and many interpretations have been based on hydrogen-bonded (HB) and non-hydrogen-bonded (NHB) species. The former are thought to contribute primarily to the lower-frequency part of the stretching band, while the latter would play a major role in determining its high-frequency portion. Very recently, Yang and Skinner[7] reported a study of light water using the same coupled classical/quantum approach[8] adopted to study dilute mixtures, and they discussed the IR band in terms of coherent vibrational energy transfers.

Here, we investigate the IR stretching band of neat, heavy water with an approach complementary to that of ref 7. We carried out ab initio molecular dynamics (AIMD) simulations and computed maximally localized Wannier functions[9] (MLWFs) to obtain IR spectrum. We show that the complex features of the broad IR stretching band cannot be simply ascribed to HB and NHB species, as in the case of dilute mixtures. When using a geometrical definition of H-bonds, we find that intermolecular dipolar correlations of both HB and NHB species contribute to the IR band over the entire frequency range. The shape of the band, with its shoulders and maximum, arises from intra- and intermolecular correlations involving molecules in the first and second coordination shells. Furthermore, the band shape can be interpreted in terms of dipolar correlation originating from distinct, electronic contributions.

We performed AIMD simulations using the Qbox code,[10] with a cubic cell containing 96 D_2O molecules. The electronic degrees of freedom were treated within density functional theory (DFT), using the Perdew−Burke−Ernzerhof[11] (PBE) approximation of the exchange correlation energy, and they were optimized at every MD step (Born−Oppenheimer (BO) dynamics). We adopted a plane wave basis set and norm-conserving pseudopotentials,[12,13] with a kinetic cutoff of 85 Ry. We carried out simulations with a time step of 10 au in the NVE ensemble at a density of 1.082 g/cm³ and at $T = 407 \pm 16$ K. As discussed, e.g. in ref 14, these simulation conditions yield structural and diffusion properties of the liquid in good agreement with experimental results obtained at ∼300 K. Our computed radial distribution function is the same as the one obtained in ref 14, within statistical error bars. In our calculations, the liquid was equilibrated at 400 K for about 24 ps, and trajectories to compute IR spectra were collected over 20 ps. The electronic contributions to the molecular dipole moment were computed using MLWFs, evaluated at each MD step with the algorithm proposed in ref 15. Within linear response theory, the IR absorption coefficient per unit length is given by the Fourier transform of the time correlation function of the system dipole moment operator. Following refs 3 and 4, we approximate the quantum time correlation function with
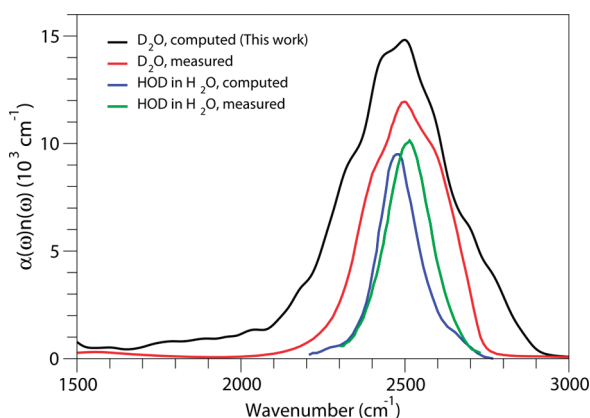
Figure 1. Calculated (black) and experimental[22] IR OD stretching bands of neat water and calculated[23] (blue) and experimental[24] (green) absorbance of diluted mixtures. The spectrum calculated in this work (black solid) has been blue-shifted by 231 cm^{-1} in order to align computed and measured peak positions. On the scale of the figure, experimental results of refs 22 and 25 are indistinguishable; likewise, experimental results from refs 24 and 26 are indistinguishable. The same overestimate of intensities found in our work was observed in refs 4 and 27.

Figure 2. Left panel: The IR stretching band of neat D_2O (black) is compared with the IR activity originating from intermolecular contributions (blue) and the OD bond power spectrum originating from intermolecular contributions (red). Right panel: The IR stretching band of neat D_2O (black) is compared with the IR activity originating from intramolecular contributions (blue) and the OD bond power spectra originating from intramolecular contributions, autocorrelation (green) and the cross-correlation between OD bonds on the same molecule (red).

the classical one, and we adopt a so-called quantum correction factor[16] obtained within the harmonic approximation; this leads to the expression

$$\alpha(\omega) = \frac{2\pi\omega^2\beta}{3cVn(\omega)} \int_{-\infty}^{\infty} dt \, e^{-i\omega t} \langle \sum_{ij} \mu_i(0) \cdot \mu_j(t) \rangle \quad (1)$$

Here, $n(\omega)$ is the refractive index, V is the volume, and $\beta = 1/k_BT$ is the inverse temperature. The molecular dipole moment is defined by $\mu_i = r_{D_1}^i + r_{D_2}^i + r_O^i - 2\sum_{c=1}^4 r_{W_c}^i$, where $r_{D_1}^i$, $r_{D_2}^i$, and r_O^i are the nuclear coordinates of ith molecule, respectively, and $r_{W_c}^i$, $c = 1,4$, are four corresponding Wannier centers. Equation 1 combined with Car–Parrinello MD,[17,18] has been successfully applied to study IR spectra of ice and bulk and confined water.[3,4,19,20] We note that different quantum correction factors have been used by different authors; for example, in the mixed classical–quantum model for dilute mixtures used by Skinner's group, a quantum correction factor in the harmonic approximation was employed using the Schofield prescription.[21] Paesani et al. used instead a correction factor consistent with the adiabatic centroid molecular dynamics (CMD) approximation of the quantum mechanical dipole–dipole correlation function.[6]

The computed IR OD stretching band is compared with experiments[22,24] in Figure 1, where results of calculations for dilute mixtures[23] are also shown. Overall, our agreement with experiment is satisfactory; the positions of the band maxima corresponding to hindered translations, librations, bending, and stretching modes are 215(186), 522(486), 1173(1209), and 2267(2498) cm^{-1}, respectively, where wavenumbers in parentheses are experimental values.[22] The statistical uncertainty on the stretching band peak position is 25 cm^{-1}. The relative intensities of all peaks compare well with experiment[22] (at variance with results obtained using the Schofield quantum correction factor that yields an intensity of the IR stretching band in excellent agreement with experiment but a rather poor
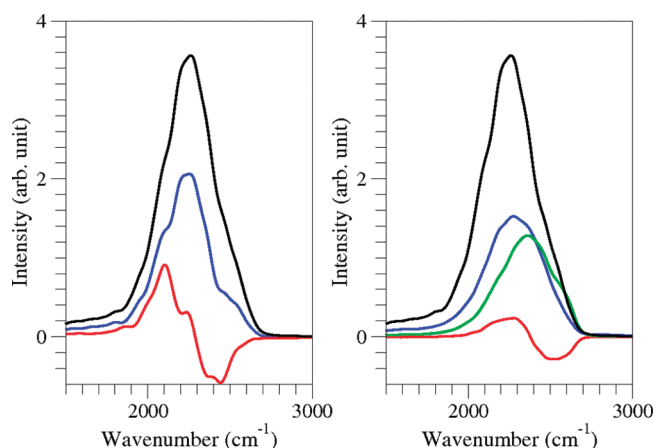
agreement for relative intensities). Although the use of BO-AIMD yields a stretching band maximum in moderately better agreement with experiments than Car–Parrinello approaches,[2−4] a non-negligible red shift (~230 cm^{-1}) with respect to the measured band maximum remains. Furthermore, the inclusion of deuteron quantum effects could increase this error by an amount varying from 10−15 cm^{-1}[6] to 70 cm^{-1}.[28] These estimates have been obtained by comparing MD and CMD results, and the latter are currently under debate.[29]

Most of the error on the peak position of the computed band arises from the use of the approximate PBE functional. On the basis of calculations carried out for the water monomer and dimer, we estimate the PBE error on stretching frequencies to be on the order of ~150 cm^{-1}. In addition to errors introduced by the use of the PBE functional, we estimate errors of the order of 50 cm^{-1} on the stretching modes and of 15 cm^{-1} on the bending modes arising from our basis sets (number of plane waves) and the use of pseudopotentials. Although the kinetic energy cutoff used here yields fully converged structural properties (e.g., pair-correlation functions), it does introduce a small error on vibrational frequencies.

Despite the red shift of our computed peak position (Figure 1), the width and shape of the IR stretching band are in good agreement with those from experiments. As found also in refs 4 and 27, the computed width at half-maximum is slightly larger than that in the experiment of ref 22, and the band is much wider than the corresponding one in dilute mixtures[23] (see Figure 1). In addition, the band of neat water is much more structured, with two clear shoulders on opposite sides of the maximum. These differences in width and shape clearly hint at the importance of intermolecular contributions to the IR spectrum of neat water, compared to that of dilute mixtures, and these contributions are discussed next.

Figure 2 shows intra- and intermolecular contributions to the IR spectrum, defined as in ref 4, compared with the OD

bond length power spectrum. This is defined as

$$I_{OD}(\omega) = \int_{-\infty}^{\infty} dt \, e^{-i\omega t} \langle \sum_{ij} d_{OD}^i(0) \cdot d_{OD}^j(t) \rangle \qquad (2)$$

This quantity includes both auto- and cross-correlations, and these can be evaluated separately by appropriately selecting the indexes of the summation in eq 2. The intermolecular OD stretching modes are correlated in the red frequency region of the band and anticorrelated in the blue region, and clear correspondences can be drawn between each peak of the ionic power spectrum ($\sim$2100, $\sim$2250, and $\sim$2450 cm^{-1}) and those in the intermolecular contributions to the IR stretching band. We note that intermolecular cross-correlations greatly contribute to the broadening of the IR stretching band of water in the condensed phase, and in particular, they constitute the major contributions to the low-frequency region of the band. We decompose the intramolecular component of the OD power spectrum into two terms, one arising from the OD bond length autocorrelation and the other one from the cross-correlation between OD bonds on the same molecule (right panel, Figure 2). The latter term displays two peaks corresponding to positive and negative correlations (in the upper part of the band), respectively, and is reminiscent of molecular symmetric and antisymmetric modes observed in the gas phase. However, the difference between the location of the two peaks (250 cm^{-1}) is about twice as large as that in the gas phase, showing the key effect of the condensed phase environment on the molecular properties of the liquid. The autocorrelation of the OD stretching mainly contributes to the high frequencies of the IR stretching band. The total ionic intramolecular OD stretching is blue-shifted with respect to the IR band arising from intramolecular contributions, as a consequence of electronic correlations and screening effects.

In order to investigate in detail electronic contributions to the IR activity of water, we define the power spectra of the stretching correlation function between oxygen and the centers of the MLWFs constructed from valence electron wave functions

$$I_{OW_c}(\omega) = \int_{-\infty}^{\infty} dt \, e^{-i\omega t} \langle \sum_{ij} d_{oxy-W_c}^i(0) \cdot d_{oxy-W_c}^j(t) \rangle \quad (3)$$

where $d_{oxy-W_c}^i$ is the distance between oxygen and the centers of the MLWFs of the *i*th water molecule. Two MLWFs are centered along OD bonds, and we call them bond pair (BP) orbitals (using a language similar to that of molecular orbitals). The other two are approximately centered on symmetric tetrahedral sites, and we call these lone pair (LP) orbitals. The four centers of the MLWFs of a water molecule are shown in the inset of Figure 3. In the left panel of Figure 3, we show the power spectra of oxygen-BP and oxygen-LP stretching correlation functions and compare them with the full IR spectrum. Our results show that the electronic fluctuations of BP and LP orbitals provide different contributions to the IR activity of the liquid. BP correlations can be related to all three features of the IR stretching band but dominate its high-frequency region. The contribution of LP orbitals is instead prominent at lower frequencies, and there is no LP response above 2500 cm^{-1}. Another interesting comparison can be
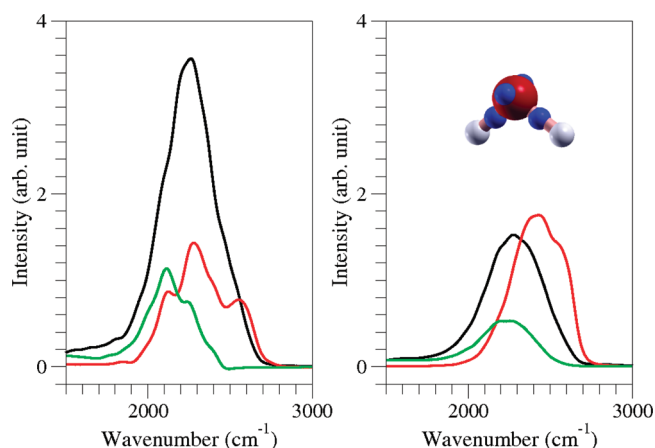

Figure 3. Left panel: The IR stretching band of neat D$_2$O (black) is compared with the IR activity originating from oxygen-BP (red) and oxygen-LP (green) correlations (BPs denotes bond pairs, and LPs denotes lone pairs). Right panel: The IR activity originating from intramolecular contributions (black) is compared with the IR activity originating from intracorrelations of oxygen-BPs (red) and oxygen-LPs (green). The inset shows the positions of the centers of maximally localized Wannier functions in a water molecule. The two orbitals centered close to the OD bonds are BP orbitals; the other two are LP orbitals.

drawn between intramolecular IR activity and the corresponding contributions of BPs and LPs. This is presented in the right panel of Figure 3. The intramolecular charge fluctuations of LPs correspond to the feature of the IR band arising from intramolecular correlations. On the other hand, the intramolecular fluctuations of BPs correspond to the features of the intramolecular ionic stretching vibrations (high-frequency part of the IR stretching band).

While BP orbitals are centered on OD bonds and are screened from the environment by the presence of the ionic charges, LP orbitals are mainly participating in H-bonding and thus are more sensitive to the intermolecular environment. As a consequence, the LP response occurs in the low-frequency region of the IR stretching band. We note that intramolecular LP fluctuations display a maximum corresponding to the position of the intramolecular part of the IR stretching band, and this is red-shifted with respect to the intramolecular ionic vibrational peak maximum shown in Figure 2, right panel.

The analysis of ionic and electronic contributions to the IR activity of water shows that intermolecular interactions play a key role in shaping the OD stretching band. Interestingly, we also find that these intermolecular interactions, in both the red and blue region of the OD stretching band, originate from interactions between molecules beyond the first coordination shell. This is shown in Figure 4, where we report the intermolecular contributions of molecules within the first ($d_{OO} < 3.35$ Å) and second ($d_{OO} < 5.6$ Å) coordination shells compared to the total intermolecular contribution to the IR spectrum. In the case of diluted mixtures, it was reported that at least 10 molecules surrounding HOD are necessary to reproduce the correct IR line shapes,[28] and vibrational correlation was analyzed in terms of electric field fluctuation.[30] These results indicate that simulations of the vibrational spectrum of liquid water based on small clusters may miss
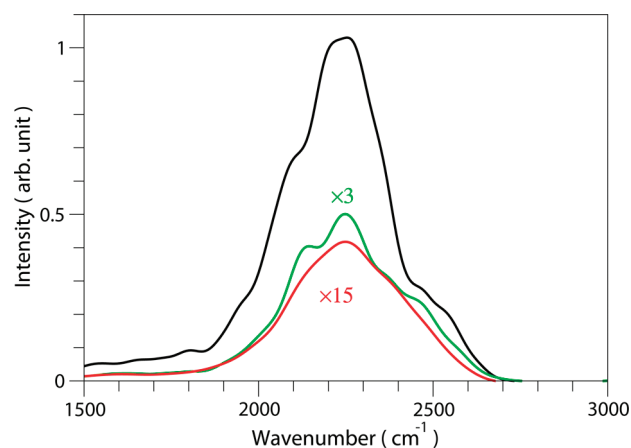
Figure 4. The intermolecular contributions to the IR stretching band of neat D_2O (black) are separated into contributions from molecules within the first (red) and second (green) coordination shells.
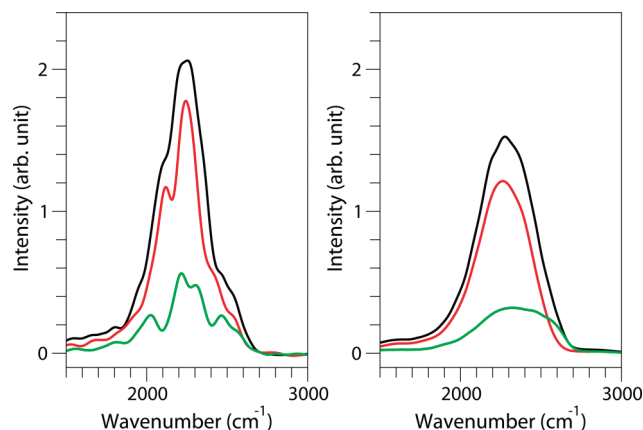

Figure 5. Left panel: The intermolecular contributions to the IR stretching band of neat D_2O are separated into those originating from HB (red) and NHB (green) species. Right panel: The intramolecular contributions to the IR stretching band of neat D_2O are separated into those originating from HB (red) and NHB (green) species.

important contributions to the IR spectrum, in addition to being affected by possible electronic surface effects.

We now turn to the discussion of the IR stretching band in terms of HB and NHB molecules, that is, of the concept used to interpret the IR band of dilute mixtures.[31,32] For simplicity, we adopt a geometrical criterion to define a H-bond in liquid water; the O–O distance is less than 3.35 Å, and the angle between the intermolecular O–O direction and the OH bond direction is less than 30°. The average population ratio of HB and NHB subensembles is about 2:1, and the average H-bonding coordination number is 3.6. Following this definition, for every simulation time frame, we define a HB subensemble, containing all of the molecules that form four H-bonds, and a NHB subensemble, containing all of the remaining molecules. We then compute the total dipole moment of each subensemble, so as to decompose the IR signal into HB and NHB contributions. These are shown in Figure 5, which displays inter- and intramolecular components on the left- and right-hand side panels,

respectively. Both intermolecular interactions of HB and NHB subensembles contribute to the IR stretching band over the entire frequency range. However, the contribution of the HB subensemble has a pronounced peak on the red side of the band and a less pronounced shoulder in the blue region. The intermolecular interaction of the NHB subensemble shows instead an equal contribution to the red and blue sides of the spectrum. The intramolecular IR contribution of the NHB subensemble (right-hand side panel in Figure 5) extends to a frequency above 2500 cm^{-1} and is blue-shifted with respect to the contribution of the HB part. Although NHB molecules contribute to the high-frequency part of the IR stretching band, their signal is not sufficient to generate clear, distinctive features, such as high-frequency shoulders or peaks. We emphasize that broken H-bonds are transient states with a computed lifetime of several hundreds femtoseconds, as suggested in ref 31.

In summary, we have provided a detailed interpretation of the complex shape and features of the IR stretching band of neat, heavy water based on AIMD. We have shown that intermolecular contributions play a key role in determining the line shape, and these contributions are long-ranged, extending to the second coordination shell. Our findings on the intricate interplay between intra- and intervibrational couplings are in agreement with the conclusions of ref 7. Our results indicate that while an interpretation of the IR stretching band in terms of HB and NHB species may be appropriate in the case of dilute mixtures, for neat water, there are no specific features that can be clearly ascribed to HB and NHB molecules. Our analysis also points at the specific role of electrons in shaping the IR stretching band; in a molecular orbital picture, we find that so-called BP orbitals give predominant contributions to the high-frequency region of the band, while LP orbitals (most sensitive to the liquid environment) mainly contribute to the low-frequency region. We note that the general analysis inferred from our simulations is not affected by the red shift of the computed IR stretching band peak with respect to experiment. Overall, our results support the picture of a continuous dynamics in neat water, with hydrogen bonds being transient states with lifetimes of several hundred femtoseconds, in agreement with the interpretation of time-resolved pump and probe spectroscopy.[31] Finally, we note that our results will be useful to interpret IR and Raman spectra of ionic solutions,[33] and work is in progress to analyze data for simple ions in heavy water.

AUTHOR INFORMATION

Corresponding Author:
*To whom correspondence should be addressed. E-mail: cuizhang@ucdavis.edu.

REFERENCES

(1) Roberts, S. T.; Ramasesha, K.; Tokmakoff, A. Structural Rearrangements in Water Viewed Throught Two-Dimentional Infrared Spectroscopy. *Acc. Chem. Res.* **2009,** *42,* 1239–1249.

(2) Silvestrelli, P. L.; Bernasconi, M.; Parrinello, M. Ab Initio Infrared Spectrum of Liquid Water. *Chem. Phys. Lett.* **1997,** *277,* 478–482.

(3) Sharma, M.; Resta, R.; Car, R. Intermolecular Dynamical Charge Fluctuations in Water: A Signature of the H-Bond Network. *Phys. Rev. Lett.* **2005,** *95,* 187401.

(4) Chen, W.; Sharma, M.; Resta, R.; Galli, G.; Car, R. Role of Dipolar Correlations in the Infrared Spectra of Water and Ice. *Phys. Rev. B* **2008,** *77,* 245114.

(5) Auer, B. M.; Skinner, J. L. Water: Hydrogen Bonding and Vibrational Spectroscopy, in the Bulk Liquid and at the Liquid/Vapor Interface. *Chem. Phys. Lett.* **2009,** *470,* 13–20.

(6) Paesani, F.; Xantheas, S. S.; Voth, G. A. Infrared Spectroscopy and Hydrogen-Bond Dynamics of Liquid Water from Centroid Molecular Dynamics with an Ab Initio-Based Force Field. *J. Phys. Chem. B* **2009,** *113,* 13118–13130.

(7) Yang, M.; Skinner, J. L. Signatures of Coherent Vibrational Energy Transfer in IR and Raman Line Shapes for Liquid Water. *Phys. Chem. Chem. Phys.* **2010,** *12,* 982–991.

(8) Auer, B. M.; Skinner, J. L. IR and Raman Spectra of Liquid Water: Theory and Interpretation. *J. Chem. Phys.* **2008,** *128,* 224511.

(9) Marzari, N.; Vanderbilt, D. Maximally Localized Generalized Wannier Functions for Composite Energy Bands. *Phys. Rev. B* **1997,** *56,* 12847–12865.

(10) *Qbox home page.* http://eslab.ucdavis.edu/software/qbox (2010).

(11) Perdew, J. P.; Burke, K.; Ernzerhof, M. Generalized Gradient Approximation Made Simple. *Phys. Rev. Lett.* **1996,** *77,* 3865–3868.

(12) Hamann, D. R. Generalized Norm-Conserving Pseudopotentials. *Phys. Rev. B* **1989,** *40,* 2980–2987.

(13) Kleinman, L.; Bylander, D. M. Efficacious Form for Model Pseudopotentials. *Phys. Rev. Lett.* **1982,** *48,* 1425–1428.

(14) Schwegler, E.; Grossman, J. C.; Gygi, F.; Galli, G. Towards an Assessment of the Accuracy of Density Functional Theory for First Principles Simulations of Water. II. *J. Chem. Phys.* **2004,** *121,* 5400–5409.

(15) Gygi, F.; Fattebert, J. L.; Schwegler, E. Computation of Maximally Localized Wannier Functions Using A Simultaneous Diagonalization Algorithm. *Comput. Phys. Commun.* **2003,** *155,* 1–6.

(16) Ramírez, R.; López-Ciudad, T.; Kumar, P. P.; Marx, D. Quantum Corrections to Classical Time-correlation Functions: Hydrogen Bonding and Anharmonic Floppy Modes. *J. Chem. Phys.* **2004,** *121,* 3973–3983.

(17) Car, R.; Parrinello, M. Unified Approach for Molecular Dynamics and Density-Functional Theory. *Phys. Rev. Lett.* **1985,** *55,* 2471–2474.

(18) Sharma, M.; Wu, Y.; Car, R. Ab Initio Molecular Dynamics with Maximally Localized Wannier Functions. *Int. J. Quantum Chem.* **2003,** *95,* 821–829.

(19) Sharma, M.; Donadio, D.; Schwegler, E.; Galli, G. Probing Properties of Water under Confinement: Infrared Spectra. *Nano Lett.* **2008,** *8,* 2959–2962.

(20) Donadio, D.; Cicero, G.; Schwegler, E.; Sharma, M.; Galli, G. Electronic Effects in the IR Spectrum of Water under Confinement. *J. Phys. Chem. B* **2009,** *113,* 4170–4175.

(21) Lawrence, C. P.; Skinner, J. L. Vibrational Spectroscopy of HOD in Liquid D_2O. II. Infrared Line Shapes and Vibrational Stokes Shift. *J. Chem. Phys.* **2002,** *117,* 8847–8854.

(22) Max, J.-J.; Chapados, C. Isotope Effects in Liquid Water by Infrared Spectroscopy. III. H_2O and D_2O Spectra from 6000 to 0 cm^{-1}. *J. Chem. Phys.* **2009,** *131,* 184505.

(23) Schmidt, J. R.; Roberts, S. T.; Loparo, J. J.; Tokmakoff, A.; Fayer, M. D.; Skinner, J. L. Are Water Simulation Models Consistent with Steady-state and Ultrafast Vibrational Spectroscopy Experiments? *Chem. Phys.* **2007,** *341,* 143–157.

(24) Park, S.; Kwak, K.; Fayer, M. D. Ultrafast 2D-IR Vibrational Echo Spectroscopy: a Probe of Molecular Dynamics. *Laser Phys. Lett.* **2007,** *4,* 704–718.

(25) Bertie, J. E.; Ahmed, M. K.; Eysel, H. H. Infrared Intensities of Liquids. 5. Optical and Dielectric Constants, Integrated Intensities, and Dipole Moment Derivatives of H_2O and D_2O at 22 ^{o}C. *J. Phys. Chem.* **1989,** *93,* 2210–2218.

(26) Asbery, J. B.; Steinel, T.; Stromberg, C.; Corcelli, S. A.; Lawrence, C. P.; Skinner, J. L.; Fayer, M. D. Water Dynamics: Vibrational Echo Correlation Spectroscopy and Comparison to Molecular Dynamics Simulations. *J. Phys. Chem. A* **2004,** *108,* 1107–1119.

(27) Lee, H.-S.; Tuckerman, M. E. Dynamical Properties of Liquid-Water from Ab Initio Molecular Dynamics Performed in the Complete Basis Set Limit. *J. Chem. Phys.* **2007,** *126,* 164501.

(28) Paesani, F.; Voth, G. A. A Quantitative Assessment of the Accuracy of Centroid Molecular Dynamics for the Calculation of the Infrared Spectrum of Liquid Water. *J. Chem. Phys.* **2010,** *132,* 014105.

(29) Ivanov, S. D.; Witt, A.; Shiga, M.; Marx, D. Communications: On Artificial Frequency Shifts in Infrared Spectra Obtained from Centroid Molecular Dynamics: Quantum Liquid Water. *J. Chem. Phys.* **2010,** *132,* 031101.

(30) Fecko, C. J.; Eaves, J. D.; Loparo, J. J.; Tokmakoff, A.; Geissler, P. L. Ultrafast Hydrogen-Bond Dynamics in the Infrared Spectroscopy of Water. *Science* **2003,** *301,* 1698–1702.

(31) Eaves, J. D.; Loparo, J. J.; Fecko, C. J.; Roberts, S. T.; Tokmakoff, A.; Geissler, P. L. Hydrogen Bonds in Liquid Water are Broken only Fleetingly. *Proc. Natl. Acad. Sci. U.S.A.* **2005,** *102,* 13019–13022.

(32) Corcelli, S. A.; Skinner, J. L. Infrared and Raman Line Shapes of Dilute HOD in Liquid H_2O and D_2O from 10 to 90 °C. *J. Phys. Chem. A* **2005,** *109,* 6154–6165.

(33) Schmidt, D. A.; Scipioni, R.; Boero, M. Water Solvation Properties: An Experimental and Theoretical Investigation of Salt Solutions at Finite Dilution. *J. Phys. Chem. A* **2009,** *113,* 7725–7729.